Hydrogen Storage Systems for Transportation Application

FINAL

Ted Yu, David B. Chang, and Reza Toossi
California State University Long Beach

METRANS contract number 03-13

June 16, 2005

METRANS Transportation Center
USC CSULB

Disclaimer

The contents of this report reflect the views of the authors, who are responsible for the facts and the accuracy of the information presented herein. This document is disseminated under the sponsorship of the Department of Transportation, University Transportation Centers Program, and California Department of Transportation in the interest of information exchange. The U.S. Government and California Department of Transportation assume no liability for the contents or use thereof. The contents do not necessarily reflect the official views or policies of the State of California or the Department of Transportation. This report does not constitute a standard, specification, or regulation.

Disclosure

Project was funded in entirety under a contract to California Department of Transportation.

Acknowledgments

The authors would like to thank the United States Department of Transportation, California Department of Transportation, and METRANS for their interest and provision of grant support to make this project possible. We would also like to thank Roy Ganzer and team at Mechanic Refrigeration Company for their invaluable technical and operational support during the activation of the experimental system.

Abstract

The binding energy per hydrogen atom is calculated versus the surface density of hydrogen molecules on graphite using mathematical modeling that takes into account the cooperative effect of neighboring carbon atoms and hydrogen molecules. A staged approach is followed with four simple models in order to gain insight into the physics of the binding. The effort was prompted by both the large range of estimates in the published literature, and by the importance of the binding energy in determining amount of hydrogen that can be stored in a given weight of graphitic material. The storage capacity is exquisitely sensitive to the value of the binding energy, depending exponentially (through a Boltzmann factor) on the energy.

As a first approximation, we estimated the binding energy following the dielectric dispersion formalism developed by Landau and Lifshitz (1969), i.e. the binding energy of two interacting systems is estimated from the zero point energies of the two systems as a function of their distance of separation.

The advantage of calculating the binding energy in this way is that it takes into account collective (cooperative) effects when several hydrogen molecules are present. Past work on the calculation of van der Waals forces has shown that the binding energy for a collection of molecules is not simply the sum of the binding energies of pairs of molecules considered individually. In an ensemble of interacting molecules the molecules behave cooperatively to enhance the interactions. This appears to be especially pronounced when one of the systems is conducting.

In our approach, we have compared the zero point energies of a collection of hydrogen molecules separated at a large distance from a piece of graphite with the zero point energies when the hydrogen molecules are juxtaposed to the graphite. The results indicate that the binding energies of hydrogen are strongly dependent on the surface density of the hydrogen bound to the graphite, with the binding energy per hydrogen molecule increasing as the surface density of hydrogen on the graphite increases.

Table of Contents

List of Figures

List of Tables

Notation

$a_{Langmuir}$ first coefficient in Langmuir isotherm equation
$b_{Langmuir}$ second coefficient in Langmuir isotherm equation
eV electron volt (1.6×10^{-19} J)
E Electric field
$E(\omega,\beta)$ blackbody function
h Planck's constant (6.626×10^{-34} J.s)
$h/2\pi$ Normalized Planck's constant (1.5443×10^{-34} J.s
H Hamiltonian
$H^{(o)}$ Unperturbed Hamiltonian
$F_i(t)$ External force
m mass of hydrogen molecule
Q_i System observable
$G_{ij}(\omega)$ correlation function of Q_i and Q_j
$^{(s)}G_{ij}(\omega)$ symmetric portion of $G_{ij}(\omega)$
$^{(a)}G_{ij}(\omega)$ antisymmetric portion of $G_{ij}(\omega)$
k_B Boltzmann's constant (1.38×10^{-23} J/K)
k wavenumber (m^{-1})
k_{max} maximum wavenumber (m^{-1})
K force constant of harmonic oscillator
M mass of harmonic oscillator
m_e Electron rest mass (9.11×10^{-31} kg)
n Volume number density of hydrogen molecules (m^{-3})
N Surface number density of hydrogen molecules (m^{-2})
N_s Saturation number density of hydrogen molecules (m^{-2})
P pressure of hydrogen (N/m^2)
T temperature
V van der Waals adsorption energy
w Thickness of hydrogen sheet (m)
x harmonic oscillator coordinate
$Y_{ij}(\omega)$ response function relating $\alpha_j(\omega)$ to $\gamma_i(\omega)$
$4\pi\alpha$ Contribution of pi electrons to ε
$\alpha_j(\omega)$ time Fourier transform of $\langle d Q_i/dt \rangle$
β $1/k_BT$
ε Dielectric constant
$\varepsilon_\perp$ Dielectric constant of graphite perpendicular to conducting plane
ε Dielectric constant of graphite parallel to conducting plane
ε_H Dielectric constant of hydrogen molecules
ε_C Dielectric constant of (isotropic) carbon insulator
ε_F Dielectric constant for fictitious isotropic conductor with same plasma frequency as carbon
$\gamma_j(\omega)$ time Fourier transform of $F_i(t)$
γ wavenumber in graphite perpendicular to graphite planes
υ damping frequency of harmonic oscillator
φ Electric potential (volts)
ω_o natural oscillation frequency of harmonic oscillator
ω_{CC} Plasma frequency of 4 2s and 2p electrons in carbon (radians/sec)
ω_C Plasma frequency of 3 core sigma electrons in graphite (radians/sec)
ω_{CO} Natural oscillation frequency of 3 core sigma electrons in graphite (radians/sec)
ω_p Plasma angular frequency of. pi electrons in graphite (radians/sec)
ω_H Plasma frequency of hydrogen molecules (radians/sec)
ω_{HO} Natural oscillation frequency of electrons in hydrogen molecule (radians/sec)
ω Frequency of a normal mode (radians/s

1. Introduction

Hydrogen is a low molecular weight, renewable and environmentally friendly energy source. Its exothermic reaction with oxygen yields water in a simple reaction: $H_2 + 1/2O_2 \Leftrightarrow H_2O$. Oxygen is readily available in air and only hydrogen needs to be stored to harness its energy. In addition, the water product can be readily expelled into the environment with little consequence to the users and their environment. The reactants may be combusted as conventional fossil fuel, but as the efficiency of combustion is limited, a greater efficiency may be harnessed through a fuel cell. Fuel cells are electrochemical devices that convert chemical energy directly into electricity.

Due to the low molecular weight of hydrogen, it would seem an ideal fuel. However, hydrogen is a gas at room temperature and has a very low density typical of gases, and takes up a large volume to store. In order for hydrogen to be a viable energy source, and competitive with fossil fuel, technologies need to be developed to reduce the amount of volume hydrogen takes up. Current technologies include compressed gas, liquefaction, metal hydride, and physisorption.

Physisorption is an area of research interest because it is the least mature technology that possibly has the greatest potential. It involves the adsorption of hydrogen through van der Waals binding forces on typically a carbon material with high surface areas. There has been much discussion recently about the use of carbon nanostructures as an efficient hydrogen storage mechanism [Atkinson, 2002]. Several reports indicate these materials have high hydrogen storage capacities at room temperatures. Other reports suggest the room temperature storage capacities are near zero weight percent. The discrepancies of the reported storage capacities may be due to the different methods of measuring weight percent, as well as the vast variety of carbon nanostructure materials with different geometrical configurations that are under research and development. In addition, modifications such as doping with alkali metals can further enhance its adsorption properties.

The present model shows an alternative method of calculating the binding energy of hydrogen adsorption by graphite, by approximating the binding energy of physical adsorption between a sheet of graphite and a sheet of hydrogen molecules. The physical adsorption occurs by the lower overall electrostatic zero point energies that occurs when the two sheets are interposed; as opposed to the higher overall energy when the two sheets are independent. Unlike previous models [Wang, 1999], the present model takes into account the cooperative effect of the entire sheet of hydrogen molecules rather than measuring just an individual hydrogen molecule's attraction to an individual carbon.

2. Background

There has been much discussion recently about the use of carbon nanostructures as an efficient hydrogen storage mechanism. Several reports indicate these materials have high hydrogen storage capacities at room temperatures. Other reports suggest the room temperature storage capacity of near zero percent. The increasing interest in hydrogen as a fuel prompts a need for a greater understanding of these carbon nanostructure storage materials.

2.1 Orbital structure of graphitic carbon

Electrons that are in different energy levels differ from each other in having different probability distributions. **Atomic orbitals** represent the ways that electrons can arrange themselves in isolated, individual atoms. Carbon has 2 electrons in K shell (n=1), and 4 valence electrons in L

shell (n=2), two in 2s orbital and two in 2p orbitals, thus the electron configuration of $1s^2 2s^2 2p^2$. 1s electrons have the lowest energy levels (-308.18 eV) and are tightly bound to the nucleus by electrostatic forces. 2s electrons have slightly lower energy (-19.20 eV) than 2p electrons (-11.79 eV) and spend more of their time close to nucleus, thus they are bound more tightly to the nucleus than 2p electrons. The spatial distribution of an s electron is spherically symmetrical, whereas p electrons are found in certain directions more than in others. When atoms bond to one another, the electrons have to change their arrangement in order to accommodate the influence of other atoms (Figure 1).

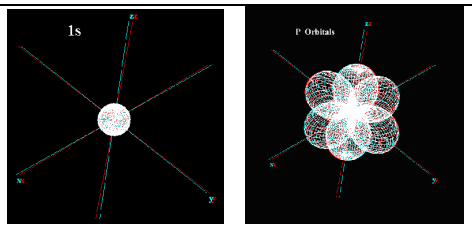

Figure 1. Atomic orbitals: s (left) and p (right) orbitals

When a carbon atom bonds to other atoms, the four orbitals in the second shell are somehow mixed together and rearranged to give four new **hybrid orbitals**. Each of the four hybrid orbitals is equivalent to the others and contains one electron. These orbitals point out from the center of the atom toward the corners of a tetrahedron (Figure 2).

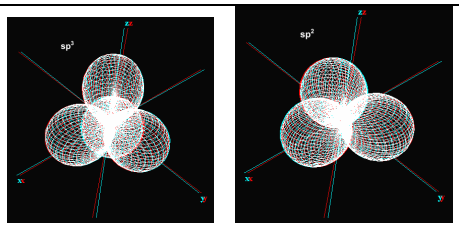
Figure 2. SP3 (left) and SP2 (right) hybrid orbitals.

Hydrogen has only one electron in its outer shell therefore it can donate only one electron to carbon by a single bond. This kind of bonding is called **sigma-bonding** and the space occupied by bonded electrons is called a bonding orbital. Figure 3a represents sigma-bond orbitals formed by sharing electrons between two S-orbitals.

When carbon bonds with other carbon atoms, the situation is more complicated. The p-orbitals can share electrons by overlapping directly between the nuclei of the atoms making the sigma-bond (Figure 3b), but may also share the leftover p-electrons. These overlap sideways to their internuclear axis, forming what are commonly called as pi-bonds. Figure 3c shows the **pi-bonding** occurring off axis and parallel to the sigma-bond which connects two carbon atoms. Depending on whether no pi-electrons, one pi-electron or two pi-electrons are shared, carbon bonds with other carbons by single, double, or triple bonds.

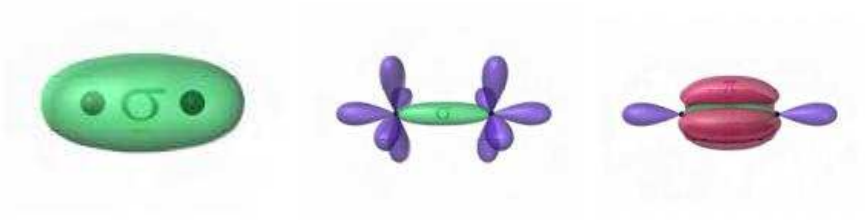
(a) (b) (c)

Figure 3. Sigma bonds formed as a result of sharing electrons by two S-orbitals (a) and two P-orbitals (b).

2.2 Properties of carbon nanostructures

The nanostructures take various forms, but have the feature that the stronger binding of hydrogen occurs in nanostructures that contain stacks of graphite.

For example, nanofibers containing graphite have been reported in which graphite platelets are evenly spaced with the planes of the graphite perpendicular to the fiber axis and separated by 3.4

angstroms. Other nanofibers [called ribbons] have the stacked graphite sheets arranged parallel to the fiber axis. Yet others have a herringbone structure, in which the graphite sheets are stacked at an angle with respect to the fiber axis. Further variants occur in that the fibers can be straight, branched, twisted or helically coiled. The particular form seems to depend in part on the type and size of catalyst used for the formation of the fiber from the decomposition of hydrocarbons or carbon monoxide. Fiber lengths as long as 100 microns with diameters in the range of 7.5-10,000 angstroms have been reported [Baker, 1997].

Carbon nanotubes represent yet another form. In single-walled nanotubes, a single roll of graphite forms a hollow cylinder of 10-20 angstrom diameter. In multi-walled nanotubes, several concentric rolls of graphite form the walls, with an overall diameter in the range of 35-1000 angstroms. The nanotubes can have lengths 5-100 times their diameter [Rodriguez, 1997]. Carbon nanoshells also form, in which polyhedral layered structures composed of multiple layers of closed shells surround a void, taking a variety of shapes and sizes.

2.3 Nanostructure storage of hydrogen

The interest in carbon nanostructures for storing hydrogen arises from their large surface areas. For example, Rodriguez and Baker [Ibid (1997)] report areas of 0.2-3000 m^2/gm, as determined from N_2 adsorption studies at 77K. The large areas, with typical interstice spacing in the range of 3.4-6.7 Angstroms, provide the potential for large amounts of hydrogen to be bound to their surfaces.

To date, the experimental data is quite mixed, with some experiments showing considerable hydrogen storage, but others showing low amounts of storage. Typical results for carbon nanotubes are in the range of 2-4 wt%, and those for nanofibers is less than 1 wt% -- although some much higher values (50-60%) have also been reported in the literature [Atkinson, 2002]

2.4 Need for an improved theoretical understanding

Theoretical estimates of hydrogen storage give results in the 4-14% wt range [Meregalli, 2001]. Although the theoretical situation leaves much to be desired, there is no agreement as to what the adsorption/desorption mechanism is – even as to whether the process is primarily chemisorption or physisorption.

Strict chemisorption – e.g. the formation of covalent bonds – would give large binding energies, and would require high temperatures for hydrogen release. On the other hand, conventional estimates of physisorption – i.e. van der Waals dispersion force bonding – would give weak binding, and would correspond to large releases of hydrogen at moderate temperatures. Either extreme is not desirable for a hydrogen storage device.

This poor understanding of the storage mechanism translates into a large uncertainty in estimating the maximum hydrogen storage capacities of carbon nanostructures.

3. Objectives

The purpose of the proposed research is to attempt to improve the state of understanding of the adsorption/desorption mechanism for hydrogen in carbon nanostructures, and thereby to improve the estimate of the hydrogen storage capacity of carbon nanostructures.

We propose to do this by taking into account the unique polarizability properties of graphite associated with the collective plasma effects of the pi electrons. From past work, we have reason

to believe that these collective effects enhance the physisorption binding forces, resulting in binding energies intermediate between chemisorption [too large] and conventional physisorption [too small] estimates.

The implications of the intermediate binding energies for a practical hydrogen storage device will also be discussed. We believe that the intermediate binding energies are just what are needed for an effective hydrogen storage device.

4. Approach

The proposed program can be divided into three sections: the first addressing the hydrogen binding energies, the second applying the hydrogen binding energies to adsorption/desorption dynamics, and the third using the results to begin an engineering design of a practical storage device.

The present model shows an alternative method to measure the binding energy for the case of hydrogen adsorption by graphite. This method approximates the binding energy by determining the collective physical adsorption between a sheet of graphite and a sheet of hydrogen molecules. The physical adsorption occurs because the overall electrostatic zero point energies that occur when the two sheets are interposed is lower than the sum of energies of the individual isolated sheets. Unlike previous models [Wang, 1999] the present model takes into account the cooperative effect of the entire sheet of hydrogen molecules, rather than measuring an individual hydrogen molecule's attraction to an individual carbon. Previous works by Chang et al. have measured the physical adsorption energy between two conducting chains [Chang, 1972], while other works have measured the physical adsorption energy between two non-conducting chains [Salem, 1962; Zwanzig, 1963; Yasuda, 1969]. The present model approximates the physical adsorption energy between two planes, one conducting and one non-conducting, and differs from previous works in the following ways. The plane model determines the two-dimensional interaction between two bodies, rather than their one-dimensional interaction. Two-dimensional interaction is a more realistic model for carbon, because carbon exists as layers of two-dimensional sheets. The modeling of two planes is an extension of the modeling of two chains. The chain model is an infinite collection of atoms along one axis, while the plane model assumes these chains are distributed on a surface. By using this approach, this model can determine the cooperative effect of a plane of hydrogen molecules lying along graphite on the physical adsorption energy.

Other than physical adsorption models, there are other approaches to measure the binding energy between graphite and hydrogen. Wang et al computed adsorption isotherms for quantum fluids [Wang, 1998]. The method is used to compute the heat of adsorption as a function of coverage for several different graphite-hydrogen potentials. They quote experimental values that after conversion from a different energy unit turns out to be between W = 0.039 eV and W = 0.055 eV.

Ye and Ahn (1999) use a chemical potential formula to estimate the binding energy. They give a "characteristic chemical potential for hydrogen physisorption" of W = 0.038 eV. Using this estimated binding energy, this group gave encouraging results: 8% by weight storage density of hydrogen at a temperature of 80 K. In another work, the group gave a low experimental storage density for carbon nanofibers of less than 1% by weight [Ahn, 1998].

An advantage to modeling the physical adsorption of two planes is that it is possible to determine how the energy varies with changing topologies of the two planes. It is possible to see what the binding energies are by varying the thickness as well as other geometrical factors in the model.

The goal of this model is to estimate the binding energy and the hydrogen storage capacity by calculating the binding energy between carbon and hydrogen and taking into account the cooperative effect a sheet of hydrogen will have when interacting with a sheet of graphite. Because a big discrepancy exists between the various models as well as the experimental results, a different modeling approach is justified to support or refute the different arguments that exist in the vast array of literature there is on this subject. The tasks proposed for this study are:

- Task 1. Literature review of binding energy of hydrogen to carbon
- Task 2. Estimate of binding energy taking into account cooperative processes in the carbon
- Task 3. Modeling of essential solid state processes determining the binding energy, from a variety of experimental data on carbon
- Task 4. Validation of model and estimate from published data with most consensual agreement
- Task 5. Engineering design of variable temperature/Arhennius plotting experimental apparatus to obtain reliable measurements of binding energy.

4.1 Hydrogen binding energies
In the first section, the objective is to calculate the binding energy of hydrogen to a graphite structure, taking into account the cooperative plasma effects of the pi electrons.

This will be done by a continuum Drude model of the graphite's pi electrons. The cooperative plasma effects will be calculated using a self-consistent field molecular orbital calculation, along the lines discussed in Chang (1970). This model lays the groundwork for site-specific binding, since the continuum treatment of the first model calculation is replaced by a site-dependent calculation in which the polarizability of a specific site is enhanced by the cooperative pi electron effects.

4.2 Adsorption/desorption dynamics
In the second section, the binding energies from the first section will be used to predict the parameter dependence of desorption/adsorption curves.

This will also be done by treating the graphite structure as providing an "effective work function" for hydrogen molecules, using the result from the first (continuum Drude) model described in Section 5.1. Adsorption/desorption curves can then be estimated by an analogue of the Richardson-Dushman equation for electron emission from electrodes. The result of this section should be estimates of the parameter dependences required for designing a practical hydrogen storage device.

4.3 Engineering design
This section uses the results generated in the two previous studies to do a preliminary engineering design of a practical storage device. In addition, a sanity check is performed to be sure that the results are in fair agreement with published data.

5. Enhanced hydrogen binding energies from cooperative plasma effects

As described above, the proposed work is based on the hypothesis that the cooperative plasma effects in the graphite structures should enhance physisorption by increasing the physisorption (dispersion-van der Waals) binding energies. The bases for this hypothesis are Drude's model and two papers by Dr. David Chang, a consultant on this project.

5.1 Drude's Model

In an attempt to explain the electrical properties of insulators and conductors, Drude proposed a simple model where free electrons in conduction bands of atoms, through the action of an external electric field, traveled through matter and collided with the atoms of the lattice or other electrons causing them to accelerate. The steady state current flow was only possible when a resistive force, proportional to the velocity, was imposed. That is, electrons except for a small drift velocity are held in position by restoring forces, but set in motion by the electric field acting on them. Drude's classical model worked only when the wavelengths of electrons were small compared to other characteristic lengths, such as the mean free paths between collisions. When size of the device is small or comparable to the electron wavelength, the Drude model must be expanded to include quantum effects. This condition is very unlikely in metals, but more plausible in semiconductors in which electrons have much smaller momentums. The Drude model and related equations are described in detail elsewhere [Slater, 1967].

A simple Drude model for dielectrics involves oscillating dipoles, but no free electrons. In metals however, electric conduction is the result of free electrons accelerated by the oscillating electromagnetic fields. Briefly, the electron is treated as a spring in an oscillating electric field. If we assume both the electric field ***E*** and displacement ***x*** oscillates with frequency ω, then the equation of motion for an electron is given as:

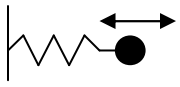

$$eE - kx = -m_e\omega^2 x$$

$$x = \frac{-e\mathrm{E}/\mathrm{m_e}}{k/m_e - \omega^2}$$

The dipole moment defined as the product of electronic charge e and displacement x:

$$p = ex = \frac{e^2\mathrm{E}/m_e}{\omega_0{}^2 - \omega^2}$$

Where **E** is the electric field, *e* is the electronic charge, m_e is the mass of electron, ω is the angular frequency of the oscillation, and $\omega_0 = (k/m)^{1/2}$ is the natural oscillation angular frequency of the bound charge in the insulator, k is the spring constant representing the restoring force proportional to the displacement of the bound electrons.

Total electric dipoles per unit volume is called polarization

$$\mathbf{P} = \mathbf{E}(\frac{Ne^2/m}{\omega_o^2 - \omega^2})$$

Where, *N* is the volume density of electrons in a solid.

It is well known that the polarizability of a conductor can be much greater than that of an insulator, because the mobility of the electrons in a conductor can result in a much larger displacement in response to a given electric field. Recalling from Maxwell's equation, the frequency-dependent dielectric constant ε (ω) which describes the polarizability of an insulator is

$$\varepsilon = 1 + \frac{4\pi P}{E} = 1 - \frac{\omega_p^2}{\omega_0^2 - \omega^2} \qquad [1a]$$

Here $\omega_p = (4\pi\, n\, e^2/m)^{1/2}$ is the plasma angular frequency of the charge species.

Free, conductive electrons behave similarly, but without the friction spring term (ω_0=0).

$$\varepsilon = 1 - \frac{\omega_p^2}{\omega^2} \qquad [1b]$$

Semiconductors, both free and bound electrons, will give additional terms in the dielectric constant so that the whole dielectric constant will be of the form.

$$\varepsilon = 1 - (\frac{4\pi\, n_o e^2/m}{\omega^2 - \omega_o^2}) - (\frac{4\pi\, n\, e^2/m}{\omega^2}) \qquad [1c]$$

Where, n_0 and n are the number densities of bound and free electrons, respectively.

Because of the absence of the ω_o in the denominator of eq. [1b] and fewer collisions between mobile electrons in a conductor compared to $\omega_{o,}$ the resulting polarization can be much greater in the conductor.[1]

5.2 A continuum estimate of the modification of binding energy due to plasma effects

The van der Waals forces responsible for the physisorption of hydrogen to graphite result from the mutual polarization of the graphite and the hydrogen. Essentially, two mutually induced oscillating dipoles interact; each induced dipole resulting from the polarization due to the oscillating electric field of the other dipole. Accordingly, anything that increases the polarization of either entity should result in a stronger force.

For a two-dimensional conductor, although the general enhancement of the dispersion force should occur, Chang [1973] applied the fluctuation-dissipation theorem to calculate the van der Waals dispersion force between two blocks of graphite and concluded that eq. [1b] is not the correct expression for determining the enhancement. However, for smaller distances of separation, the interaction between two, three-dimensional conductor blocks is due primarily to the excitation of surface plasmons, whereas for two graphite-like blocks, no surface plasmons exist, and the interaction is due to the excitation of damped charge fluctuations.

Each sheet will be treated as planar and infinite in extent, and will be characterized by a frequency-dependent Drude model dielectric function.

[1] It is interesting to note that the dispersion force cannot be calculated by looking at the $1/r^6$ interaction of a dipole with its image dipole in the conductor. Rather, the effect of the image needs to be calculated on the dispersion relation, giving both a larger force and one that drops off more slowly with distance.

For the present application this work is extended to two sheets of materials, one insulator and one conductor. Specifically, the hydrogen sheet will be treated as an insulating layer with a dielectric of the form:

$$\varepsilon_H = 1 - \omega_H^2 \, [\omega^2 - \omega_{OH}^2]^{-1} \qquad [2]$$

Where $\omega_H^2 = \frac{4\pi n_H \, e^2}{m_e}$ is the square of the "plasma frequency" of hydrogen electrons, ω is the frequency of interest, and ω_{OH} is the natural restoration frequency of the electrons in a hydrogen molecule, n_H denotes the volume density of the hydrogen molecules in the sheet, e is twice the electronic charge (since there are 2 electrons per molecule), and m_e is twice the mass of an electron. The plasma and restoration frequency can be determined from experimental data.

For the graphite sheet, the dielectric function is different for electric fields parallel to the plane of the sheet $\varepsilon_{C:}$ and for electric fields perpendicular to the plane of the sheet $\varepsilon_{C\perp}$:

$$\varepsilon_{C:} = 1 - \omega_C^2 \, [\omega^2 - \omega_{OC}^2]^{-1} - \omega_P^2/\omega^2 \qquad [3a]$$
$$\varepsilon_{C\perp} = 1 - \omega_C^2 \, [\omega^2 - \omega_{OC}^2]^{-1} \qquad [3b]$$

In these expressions, $\omega_C^2 = \frac{4\pi \, n_C \, e^2}{m_e}$ is the square of the "plasma frequency" of the core electrons, ω_{CO} is the natural restoration frequency of the core electrons, and ω_P^2 is the square of the plasma frequency of the graphite conduction electrons. As with the quantities for the hydrogen molecules, these values can be determined from experimental data.

For our purposes, we need only the frequency-dependent dielectric functions that result from the Drude model. These are listed in Table 1 below.

Table 1. Drude dielectric constants

Isotropic carbon insulator

$$\varepsilon_c(\omega) = 1 - \omega_{CC}^2 \, [\omega^2 - \omega_{CO}^2]^{-1} \qquad [4]$$

Fictitious isotropic conductor with same conductivity as graphite

$$\varepsilon_F(\omega) = 1 - \omega_F^2/\omega^2 \qquad [5]$$

Graphite

Dielectric perpendicular to graphite planes

$$\varepsilon_\perp(\omega) = 1 - \omega_C^2 \, [\omega^2 - \omega_{CO}^2]^{-1} \qquad [6a]$$

Dielectric parallel to graphite planes

$$\varepsilon_\parallel(\omega) = \varepsilon_\perp(\omega) + 4\pi\alpha \qquad [6b]$$

$$4\pi\alpha = -\omega_P^2/\omega^2 \qquad [6c]$$

Hydrogen

$$\varepsilon_H(\omega) = 1 - \omega_H^2 \, [\omega^2 - \omega_{HO}^2]^{-1} \qquad [7]$$

The numerical values of various parameters used in equations 1-3 above are estimated in the next section.

5.3 Zero point energy approach with Drude model

The approach used for estimating the binding energies consists of calculating the electrostatic normal modes of the system of interacting entities, and assigning the appropriate amplitude to each of the normal modes.

The normal modes of a system are those perturbations of the system that oscillate at some frequency natural to the system. Thus, they can be derived by assuming a disturbance of the form $\exp[-i\omega t]$ into the equations of motion, and seeing what the form of the perturbation must be to sustain the disturbance and what the resulting natural frequency must be.

A normal mode can be considered to be a giant harmonic oscillator. The allowable energy levels of a harmonic oscillator are known from quantum mechanics to be:

$$E_n = (n+ \tfrac{1}{2}) (h/2\pi)\omega \qquad [8]$$

Where $h = 6.625 \times 10^{-27}$ erg sec is Planck's constant, and ω is the angular frequency of the harmonic oscillator.

Thus, the lowest energy state of the harmonic oscillator has a "zero point" energy of

$$E_o = h\omega/4\pi \qquad [9]$$

Each of the normal modes will be assumed to have this zero point energy.

The rationale for assigning the zero point energy to each normal mode is provided by the fluctuation-dissipation theorem. A good discussion of this theorem is provided in Landau and Lifshitz (1969) and repeated in Appendix A.

In the next Section, we shall summarize the Drude model results to be used in calculating the normal mode frequencies.

5.3a Hydrogen molecule volume

We shall approximate the molecular volume by first estimating the atomic hydrogen volume, and then simply multiplying that by 2.

The radial distribution of the electron (1s ground state) about the hydrogen nucleus is:

$$a_o = h^2 [4\pi^2 m_e e^2]^{-1} = 5.29 \times 10^{-11} \text{ m}$$

Where h is Planck's constant, m_e is the electron mass, and e is the electron charge.2

We approximate the hydrogen molecule volume by

$$V_H = 2 (4\pi/3) a_o^3 = 1.24 \times 10^{-30} \text{ m}^3 \qquad [10]$$

2 For unit conversion use $k_c = 8.988 \times 10^9$ kg·m^3/C^{2}s^2 which is the Coulomb's constant.

5.3b Hydrogen plasma frequency
The plasma frequency is given by

$$\omega_H^2 = 4\pi\, n_{e,H}\, e^2/m_e \qquad [11]$$

Where $n_{e,H}$ is the number density of electrons in the molecule, and can vary between 0 and n_C. The number density can be best estimated based on the Langmuir isotherm equation

$$N/N_s = a_{Langmuir}\, P\, [1 + b_{Langmuir} P]^{-1} \qquad [12a]$$

In this expression, N denotes the surface density of hydrogen and N_s denotes the saturation surface density. For graphite with an intercarbon spacing of 1.42 angstroms, if we assume that the saturation density is the same as the surface density of carbons, then $N_s = 5.7 \times 10^{15}$ cm^{-2}.

The Langmuir coefficients are expressed in terms of the temperature T and the van der Waals adsorption energy V. Specifically,

$$a_{Langmuir} = b_{Langmuir} = h \exp(V/k_B T)[N_s (3m)^{1/2} (k_B T)^{3/2}]^{-1} \qquad [12b]$$

m denotes the mass of a hydrogen molecule. For a typical published value for V of 0.04 eV, and the pressure of 100 atmospheres and the temperature of room temperature, 300K, then $N_s = 1.7 \times 10^{14}$ cm^{-2}. Assume a monolayer of hydrogen molecules on the graphite surface. Taking the size of the hydrogen molecule to be twice the van der Waals radius of a hydrogen atom, the thickness of the monolayer is 2.6 angstroms. Thus, a surface density of 1.7×10^{14} cm^{-2} corresponds to a volume density of $n = 6.6 \times 10^{19}$ cm^{-3}. Substituting these values in equation [11], we get

$\omega_H^2 = 1.96 \times 10^{31}$ sec^{-2} [typical for a binding energy of 0.04 eV at 100 atm and 300 K] [13]
$\omega_H = 4.43 \times 10^{15}$ sec^{-1}

The value of ω_H^2 will of course vary as the surface density varies, so that a range of values will be considered in the following.

To estimate the binding energy per unit area of surface, the zero point energies of the different normal modes need to be summed over the number of normal modes per unit area. Designating a normal mode by its surface wave number k, the number of normal modes in a wave number interval $2\pi k dk$ is simply $2\pi k dk/(2\pi)^2$.

Thus, the number of normal modes per unit area to be summed over is

$$N_{nm} = \int 2\pi k dk / (2\pi)^2 = (1/4\pi)\, k_{max}^2 \qquad [14a]$$

Where the integral is taken from k = 0 to k_{max}. Since the number of normal modes per unit area must be equal to the surface density of hydrogen molecules N,

$$k_{max} = (4\pi N)^{1/2} \qquad [14b]$$

For the binding of hydrogen to the surface of a material, the electric fields responsible for the binding are large only near the surface. Thus, the normal modes that are of interest for calculating the binding energies are not the modes in the bulk of the material and of the external

space, but only those that are confined to the region of the surface. That is, the normal modes that are to be summed over are only the **surface normal modes**.

5.3c Hydrogen natural oscillation frequency

From the correspondence principle, the natural oscillation frequency corresponds to the frequency associated with the energy level transition for a non-zero dipole matrix element. For hydrogen, this occurs between the n = 1 and n=2, where n is the radial quantum number.

For hydrogen the ionization energy is 13.6 eV, which corresponds to a transition between n = 1 and n = ∞. For a transition between n=1 and n=2 we have:

$$\Delta E = (1/1^2 - 1/2^2)\ 13.6\ eV = 0.75 \times 13.6 \times 1.6 \times 10^{-19}\ J = 1.63 \times 10^{-18}\ J$$

and

$$\omega_{HO}^2 = 2.4 \times 10^{32}\ sec^{-2} \qquad [15]$$
$$\omega_{HO} = 1.55 \times 10^{16}\ sec^{-1}$$

5.3d Carbon plasma frequency

Crystalline graphite consists of parallel sheets of carbon atoms. Each sheet consists of hexagonal arrays of carbon atoms (See Figure 4). Each carbon atom is in sp2 hybridization and is connected to three neighboring atoms within a sheet by a covalent sigma bond, separating them by a distance of 1.415°A. Sheets are held together by weak Van der Waals forces, separated from each other by a distance of 3.3504°A. These sheets are staggered by half a bond length, therefore graphite configuration is repeated by a distance of twice the separation distance between adjacent sheets. The graphitic structure can be seen as repeats of carbon cells made of parallelepipeds with sides identified by the lattice parameters by a and c. The cell volume is calculated as

$$V = a^2.c.\sin(2\pi/3)$$

For graphite we have a = 2.4612 °A and c = 6.7079 °A, giving a cell volume of $35.189 \times 10^{-30}\ m^3$. There are 4 atoms of carbon in each cell so each carbon atom occupies a volume one quarter of the cell volume ($V_c = 8.797 \times 10^{-30}\ m^3$).[3]

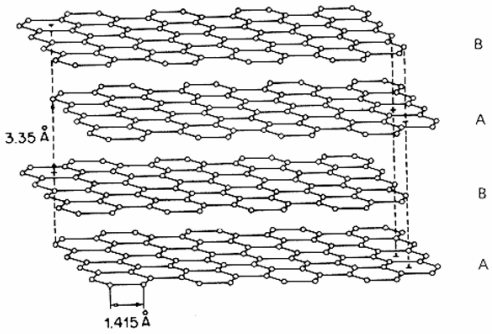

Figure 4. Crystalline structure of graphite

The ionization energies for the first four electrons in the n=2 level (2s and 2p electrons), and the first two electrons in the n=1 level (1s electron) of carbon are: 1086.5, 2352.6, 4620.5, 6222.7, 37831, and 47277 kJ/mole. Since it is much costlier energetically for the 1s electrons to

[3] Alternatively carbon atoms can be approximated as $V_C = MW/(N_{AV}.\rho)$, where ρ is x-ray density equal to 2.2670 g/cm^3.

participate in dipole transitions that it is for the 2s and 2p electrons, we can safely make the approximation that the plasma frequency of carbon is simply determined by four (4) sigma electrons occupying the volume $V_{C.}$

In that case,

$$\omega_C^2 = 4\pi\,(4/V_c)\,e^2/m_e$$
$$\omega_C^2 = 1.08 \times 10^{33}\ \text{sec}^{-2} \qquad [16]$$
$$\omega_C = 3.29 \times 10^{16}\ \text{sec}^{-1}$$

Carbon plasma frequency of sigma electrons

In graphite, there are 3 localized n = 2 (sigma) electrons per carbon atom that have orbitals in the plane of the graphite sheet. These do not participate in the conduction phenomenon. Since the plasma frequency of carbon in its insulating state has already been assumed to involve only the four n = 2 electrons, the plasma frequency of the sigma electrons is given by

$$\omega^2 = (3/4)\omega_C^{\,2}$$
$$\omega_{C,\,\sigma} = 3.08 \times 10^{16}\ \text{sec}^{-1} \qquad [17a]$$

Carbon plasma frequency of pi electrons

In graphite, there is one unlocalized n = 2 electron per carbon atom. This occupies a π-orbital that protrudes above and below the graphite sheet (See Figure 4). Pi electrons are responsible for the electrical conductivity of graphite. Accordingly,

$$\omega^2 = (1/4)\,\omega_C^2 \qquad [17b]$$
$$\omega_{C,\,\pi} = 1.90 \times 10^{16}\ \text{sec}^{-1}$$

Carbon natural oscillation frequency

To estimate ω_{0C}, we note that the zero frequency limit of the Drude expression (Equation 2) for the dielectric constant of carbon is simply

$$\varepsilon(\omega=0) = 1 + \omega_C^2/\omega_{0C}^2$$

The dielectric constant of carbon at low frequencies is given as[4]:

$$\varepsilon(\omega\rightarrow 0) = 2.5\text{-}3.0$$

Let's assume $\varepsilon(\omega\rightarrow 0) = 3$, $\omega_C^2/\omega_{0C}^2 = 2$ or $\omega_{0C}^2 = \omega_C^2/2$. This gives plasma frequency of the graphite conduction electrons:

$$\omega_{CO}^2 = 7.24 \times 10^{32}\ \text{sec}^2 \qquad [17c]$$
$$\omega_{CO} = 2.69 \times 10^{16}\ \text{sec}^{-1}$$

.

The summary of results is given in Table 2.

[4] See for example ASI Instrumentation Website at http://www.asiinstr.com/dc1.html.

Table 2. Numerical values of squared frequencies appearing in dielectric constants [(radians/sec)^2]	
ω_{CC}^2	14.4×10^{32}
ω_{CO}^2	7.24×10^{32}
ω_F^2	1.10×10^{32}
ω_C^2	10.80×10^{32}
ω_P^2	1.10×10^{32}
ω_H^2	0.20×10^{32}
ω_{HO}^2	2.40×10^{32}

6. Modeling

The objective of this model it to calculate the binding energy of a layer of hydrogen on a sheet of graphite, while taking into account cooperative effects due to the presence of multiple hydrogen molecules and multiple carbon atoms in the graphite. The approach will be to compare the sum of the zero point energies of the electrostatic surface modes of two juxtaposed dielectric sheets with that for two dielectric sheets separated by an infinite distance. The dielectric functions are chosen so that one represents a graphite sheet and the other represents a layer of hydrogen molecules.

The modeling is carried out in four easier steps:

Case 1. The van der Waals binding energy between a block of carbon in its insulating form and a block of hydrogen.

Case 2. The van der Waals binding energy between a block of carbon in its insulating form and a thin sheet of hydrogen

Case 3. The van der Waals binding energy between a block of a fictitious material with isotropic conductivity, and a thin sheet of hydrogen

Case 4. The van der Waals binding energy between a block of graphite and a thin sheet of hydrogen.

We felt that it was important to treat the thin hydrogen sheet case in three of the four cases, since the hydrogen block case is quite artificial and does not permit a realistic variation of hydrogen density. The block case applies only to condensed or liquid hydrogen, since it does not permit a larger density at the interface with carbon than in the hydrogen bulk volume itself.

The first two cases enable us to see the difference is between two blocks of material and a block and a sheet. In particular, it showed for this simple isotropic situation, why there appears to a change in the sign of the binding energy between these two cases.

The second and third cases show us what the difference is between binding to an isotropic insulator and binding to an isotropic conductor. They show that binding is larger for the isotropic conductor than for the isotropic insulator.

The fourth case gives us the desired result. It clearly displays the effect of hydrogen density in the sheet on the binding energy of each hydrogen molecule. By approaching this answer by simpler stages, insight is also provided as to why the energies calculated in our earlier work have been so large.

In each case our approach consists of comparing the zero point energies of the first configuration with the sum of the zero point energies of the latter two configurations. The difference is the desired binding energy of the hydrogen sheet to the graphite sheet.

6.1 Case 1. Interface of a block of isotropic carbon insulator with a block of hydrogen

Consider first the simple case of a block of hydrogen interfacing with a block of an isotropic carbon insulator. In accordance with the discussion of Section 2, the binding energy between the two blocks can be obtained from the zero point energies of the surface modes existing at the interface.

Before considering the surface energy at the interface of the two blocks, consider first the simpler case of the surface modes at the interface of a block of carbon and air (Section 6.1a), and the surface modes at the interface of a block of hydrogen and air (Section 6.1b). The systems treated in Sections 6.1a, 6.1b, and 6.1c are depicted in Figure 5.

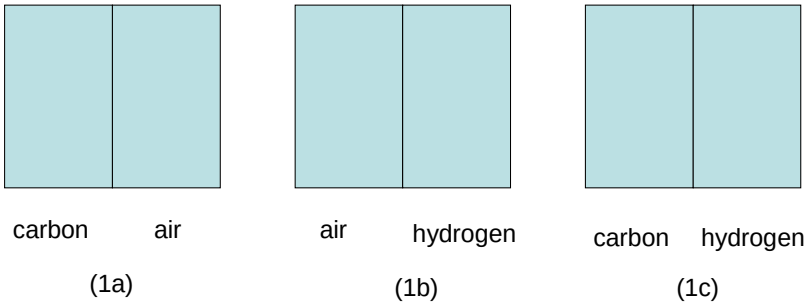

Figure 5. Blocks of (a) isotropic carbon insulator interfacing with air, (b) condensed hydrogen interfacing with air, (c) isotropic carbon insulator interfacing with condensed hydrogen

6.1a Surface mode of a block of carbon and air

In keeping with Figure 5.1a, assume that a block of carbon is separated from air by an interface at x=0, and search for electrostatic surface modes.

Assume that the electrostatic potential φ has a disturbance of the form

$$\varphi(x,y,t) = \varphi(y) \exp[i(\omega t - ky)] \qquad [18]$$

Where y is a coordinate parallel to the interface and t is the time.

The equation for the φ in each of the two regions is Laplace's equation

$$d^2\varphi/dx^2 - k^2\varphi = 0 \qquad [19]$$

For a surface mode, the relevant solutions are

$$\varphi = A \exp[kx] \qquad \text{when } x<0 \qquad [20a]$$

$$\varphi = B \exp[-kx] \qquad \text{when } x>0 \qquad [20b]$$

as these give fields that are large only near the interface.

At the interface, the boundary conditions are

$$\varphi(0-) = \varphi(0+) \qquad [21a]$$

$$\varepsilon_c \, d\varphi(0-)/dx = d\varphi(0+)/dx \qquad [21b]$$

Thus,

$$A = B$$

and

$$\varepsilon_c + 1 = 0 \qquad [22]$$

Equation [22] indicates that a surface mode exists if and only if it is possible to have

$$\varepsilon_c < 0 \qquad \text{[Necessary condition for surface mode]}$$

From the expression for ε_c from eq. [4] of Table 1, eq. [22] becomes

$$2 - \omega_{CC}^2 [\omega^2 - \omega_{CO}^2]^{-1} = 0$$

This gives as the frequency (squared) of the surface normal mode:

$$\omega^2 = \omega_{CO}^2 + \omega_{CC}^2/2 \qquad [23]$$

6.1b Surface mode of a block of hydrogen and air

For the situation depicted in Figure 5.1b, the relevant solutions are once again

$$\varphi = A \exp[kx] \qquad \text{when } x<0 \qquad [24a]$$

$$\varphi = B \exp[-kx] \qquad \text{when } x>0 \qquad [24b]$$

At the interface, the boundary conditions are

$$\varphi(0-) = \varphi(0+) \qquad [25a]$$

$$d\varphi(0-)/dx = \varepsilon_H \, d\varphi(0+)/dx \qquad [25b]$$

Thus,

$$A = B$$

and

$$\varepsilon_H + 1 = 0 \qquad [26]$$

From the expression for ε_H from eq. [7] of Table 1, eq. [26] becomes

$$2 - \omega_H^2 [\omega^2 - \omega_{HO}^2]^{-1} = 0$$

This gives as the frequency (squared) of the surface normal mode:

$$\omega^2 = \omega_{HO}^2 + \omega_H^2/2 \quad [27]$$

6.1c Surface mode between carbon and hydrogen

Next consider the situation depicted in Figure 1c, where a block of condensed hydrogen is juxtaposed to the block of carbon.

The boundary condition for this situation is

$$\varphi(0-) = \varphi(0+) \quad [28a]$$

$$\varepsilon_c d\varphi(0-)/dx = \varepsilon_H d\varphi(0+)/dx \quad [28b]$$

i.e.

$$\varepsilon_c + \varepsilon_H = 0 \quad [29]$$

For this case, ε_c and ε_H must have opposite signs. From the forms of ε_c and ε_H, this can occur only if eq. [29] has a solution for ω^2 in the range

$$\omega_{HO}^2 + \omega_H^2 < \omega^2 < \omega_{CO}^2 + \omega_{CC}^2 \quad [30]$$

$$\omega^2 = \omega_{HO}^2 + \omega_H^2/(\varepsilon_c + 1) \quad [31]$$

For the typical values shown in Table 2, we see that

$$\omega_{CC}^2 >> \omega_{HO}^2, \omega_H^2$$

Thus, for a solution close to that for a surface mode of hydrogen with air, a good approximation to eq. [30b] is obtained by substituting for ε_c the $\omega = 0$ limit $\varepsilon_c(0)$:

$$\omega^2 \approx \omega_{HO}^2 + \omega_H^2/(\varepsilon_c(0) + 1) \quad [32]$$

The solution of eq. [32] clearly outside the range of eq. [30] required for a surface mode. Thus, there is no surface mode if ω^2 has a value close to that of the surface mode of a block of hydrogen in air.

Eq. [29] may also be written

$$\omega^2 = \omega_{CO}2 + \omega_{CC}^2/(\varepsilon_H + 1) \quad [33a]$$

For ω^2 close to the value for a surface mode of carbon in air, we see from the typical values of Table 2, we see that ε_H is very close to unity. Thus, a good approximation to eq. [33a] is obtained by replacing the ω^2 in the ε_H by the zeroth order iteration value

$$\omega(0)^2 = \omega_{CO}^2 + \omega_{CC}^2/(1 + 1)$$

In that case, the approximate solution is

$$\omega^2 = \omega_{CO}^2 + \omega_{CC}^2/(\varepsilon_H(\omega(0)^2) + 1)$$

Where

$$\varepsilon_H(\omega(0)^2) = 1 - \omega_H^2 [\omega_{CO}^2 + (\omega_{CC}^2/2) - \omega_{HO}^2]^{-1}$$

Since $\omega_{CO}^2 >> \omega_H^2$,

$$\omega^2 = \omega_{CO}^2 + \omega_{CC}^2/2 + (\omega_{CC}^2\omega_H^2/4)[\ \omega_{CO}^2 + \omega_{CC}^2/2 - \omega_{HO}^2]^{-1} \qquad [33b]$$

This satisfies the surface mode existence requirement of eq. [30].

Thus, for a block of carbon juxtaposed to a block of condensed hydrogen, the surface mode that exists has practically the same zero point energy as that of carbon in air.

To summarize, the zero point energy frequencies for the surface modes are:

$$\omega = [\omega_{CO}^2 + \omega_{CC}^2/2]^{1/2} \qquad \text{carbon/air interface} \qquad [34a]$$

$$\omega = [\omega_{HO}^2 + \omega_H^2/2]^{1/2} \qquad \text{hydrogen/air interface} \qquad [34b]$$

$$\omega = [\omega_{CO}^2 + \omega_{CC}^2/2 + (\omega_{CC}^2\omega_H^2/4)[\ \omega_{CO}^2 + \omega_{CC}^2/2 - \omega_{HO}^2]^{-1}]^{1/2} \qquad \text{carbon/hydrogen} \qquad [34c]$$

The frequency $\delta\omega$ to be associated with the binding energy of carbon and hydrogen is the sum of the first two frequencies [those existing when the blocks are widely separated] minus the third frequency [the surface mode frequency when the blocks are juxtaposed]:

$$\delta\omega = [\omega_{CO}^2 + \omega_{CC}^2/2]^{1/2} + [\omega_{HO}^2 + \omega_H^2/2]^{1/2} - [\omega_{CO}^2 + \omega_{CC}^2/2 + (\omega_{CC}^2\omega_H^2/4)[\ \omega_{CO}^2 + \omega_{CC}^2/2 - \omega_{HO}^2]^{-1}]^{1/2}$$

or on expanding the third term using the fact that $\omega_{CO}^2 >> \omega_H^2$

$$\delta\omega = [\omega_{HO}^2 + \omega_H^2/2]^{1/2} - (\omega_{CC}^2\omega_H^2/8)[\ \omega_{CO}^2 + \omega_{CC}^2/2 - \omega_{HO}^2]^{-1}[\omega_{CO}^2 + \omega_{CC}^2/2]^{-1/2}$$

The corresponding binding energy is practically determined by the first term in this expression. The binding energy is essentially due to the fact that the surface mode that exists when bulk hydrogen interfaces with air is eliminated when the hydrogen interfaces instead with carbon.

This has a large value. However, this is a very artificial case, since it assumes that hydrogen exists in a block rather than condensed at the carbon surface. Hence, we use this only for illustrative purposes to show the essential ingredients of calculating the frequencies of surface modes.

A more realistic case is considered in the next Section.

6.2 Case 2. A block of isotropic carbon with a thin sheet of hydrogen on a surface

A more realistic situation is that of a block of isotropic carbon insulator on one surface of which is deposited a thin sheet of hydrogen. This corresponds to hydrogen condensing on the surface of the carbon due to adsorption.

The approach to calculating the binding energy from the zero point oscillation frequencies is:

a. Determine the frequencies of the surface normal modes of carbon and air
b. Find the frequencies of the normal modes of a thin sheet of hydrogen in air

c. Determine the frequencies of the surface normal modes of carbon with a deposited thin sheet of hydrogen between it and air
d. Subtract the frequencies from the third step from the first two steps, and integrate over wave numbers to obtain the zero point energy of adhesion per unit area.

The situations for the four steps are depicted in Figure 6.

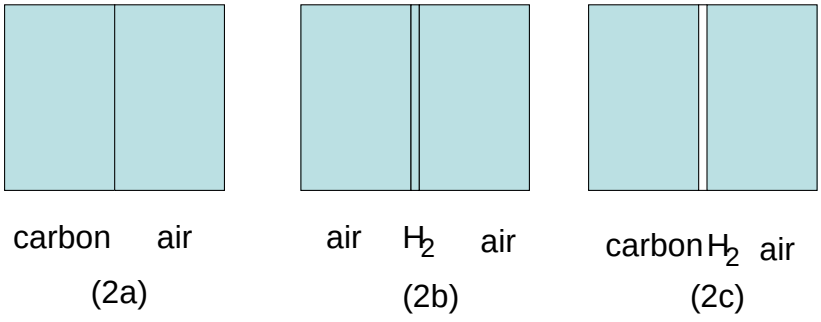

Figure 6. A block of isotropic carbon insulator in air [2a]; a thin sheet of hydrogen of width w in air [2b]; and a block of carbon insulator coated with a thin sheet of hydrogen of width w in air [2c]

6.2a Surface mode of a block of carbon and air
The calculation of the zero point frequencies for the surface modes for a block of carbon interfacing with air has already been calculated in the previous Section. The answer is given in eq.[23]

$$\omega^2 = \omega_{CO}{}^2 + \omega_{CC}{}^2/2 \qquad [[23]]$$

6.2b Two modes of a thin sheet of hydrogen in air
Next consider a thin sheet of hydrogen of width w in air.

In each region the potential φ satisfies Laplace's equation. Assuming $\varphi(x,y,t) = \varphi(y) \exp[i(\omega t - ky)]$, the surface modes of interest will have the forms

$$\varphi = A\exp[kx] \qquad x<0 \qquad [35a]$$

$$\varphi = B\cosh[kx] + C\sinh[kx] \qquad 0<x<w \qquad [35b]$$

$$\varphi = D\exp[-kx] \qquad x>w \qquad [35c]$$

The boundary conditions at the interfaces are

φ continuous [36a]

$d\varphi(0-)/dx = \varepsilon_H\, d\varphi(0+)/dx$
[36b]

$\varepsilon_H\, d\varphi(w-)/dx = d\varphi(w+)/dx$ [36c]

Since the width w of the hydrogen layer is very small, the cosh and sinh may be approximated by

$\cosh[kx] \approx 1$

$\sinh[kx] \approx kx$

With these approximations, eq. [36] then gives

$$\varepsilon_H^2 + (2/kw)\,\varepsilon_H + 1 = 0 \qquad [37]$$

To lowest order in kw, this has two solutions:

$$\varepsilon_H = -\ kw/2 \qquad \text{[odd } \varphi \text{ solution]} \qquad [38a]$$

giving

$$\omega^2 \approx \omega_{HO}^2 + \omega_H^2 - \omega_H^2\,(kw/2) \qquad \text{[odd } \varphi \text{ solution]}$$

i.e.

$$\omega \approx [\omega_{HO}^2 + \omega_H^2]^{1/2} - \omega_H^2[\omega_{HO}^2 + \omega_H^2]^{-1/2}\,(kw/4) \quad \text{[odd } \varphi \text{ solution H in air]} \qquad [38b]$$

and

$$\varepsilon_H = -\ 2/kw \qquad \text{[even } \varphi \text{ solution]} \qquad [39a]$$

which gives

$$\omega^2 \approx \omega_{HO}^2 + \omega_H^2(kw/2) \qquad \text{[even } \varphi \text{ solution]}$$

i.e.

$$\omega \approx \omega_{HO} + (\omega_H^2/\omega_{HO})(kw/4) \qquad \text{[even } \varphi \text{ solution H in air]} \qquad [39b]$$

6.2c Modifications of the three modes for hydrogen sheet on carbon

For the situation depicted in Figure 6.2c, the solutions in the three regions have the same form as before, but now the boundary conditions at the interfaces are modified slightly:

$$\varphi \text{ continuous} \qquad [40a]$$

$$\varepsilon_C d\varphi(0-)/dx = \varepsilon_H\, d\varphi(0+)/dx \qquad [40b]$$

$$\varepsilon_H\, d\varphi(w-)/dx = d\varphi(w+)/dx \qquad [40c]$$

Equation [37] is replaced by

$$\varepsilon_H^2/\varepsilon_C + (2/kw)[(1/\varepsilon_C) + 1]\,\varepsilon_H + 1 = 0 \qquad [41]$$

Solving this quadratic equation in ε_H to lowest order, this gives the two solutions originating from the thin hydrogen sheet modes

$$\varepsilon_H = -kw\,[1 + (1/\varepsilon_C)]^{-1} \qquad [42a]$$

$$\varepsilon_H = -\,(1/kw)\,[1+\varepsilon_C] \qquad [42b]$$

On the other hand, solving eq. [41] for ε_C gives a third solution originating from the carbon surface mode with air:

$$\varepsilon_C + 1 = -\,[\varepsilon_H + (\varepsilon_C/\varepsilon_H)]kw \qquad [42c]$$

Consider first the hydrogen sheet mode of eq. [42a] that corresponds to the odd φ mode of the hydrogen sheet in air. Since kw<<1, the coefficient $[1+ (1/\varepsilon_C)]^{-1}$ of kw on the RHS of the equation can be evaluated by inserting into it the frequency obtained by setting kw = 0:

$$\omega(w=0)^2 \approx \omega_{HO}^2 + \omega_H^2$$

The resulting frequency is to lowest order:

$$\omega \approx [\omega_{HO}^2 + \omega_H^2]^{1/2} - \omega_H^2 [\omega_{HO}^2 + \omega_H^2]^{-1/2} (kw/4)\, \xi \qquad \text{[odd } H_2 \text{ sheet mode]} \qquad [43a]$$

Where

$$\xi = [\omega_{HO}^2 + \omega_H^2 - \omega_{CO}^2 - \omega_{CC}^2)][\, \omega_{HO}^2 + \omega_H^2 - \omega_{CO}^2 - (\omega_{CC}^2/2)]^{-1}$$

The frequency for the odd H_2 sheet mode **decreases** with juxtaposition to the carbon.

Next, consider the hydrogen sheet mode of eq. [42b] that corresponds to the even φ mode of the hydrogen sheet in air. The solution to this equation is

$$\omega \approx \omega_{HO} + (\omega_H^2 / \omega_{HO})\, (kw/2)[1+\varepsilon_C]^{-1}$$

Again, since kw<<1, the ε_C in the coefficient of kw can be evaluated as if kw were zero, i.e. ε_C can be approximated by

$$\varepsilon_C(w=0) = 1 - \omega_{CC}^2[\omega_{HO}^2 - \omega_{CO}^2]^{-1}$$

This gives

$$\omega \approx \omega_{HO} + (\omega_H^2 / \omega_{HO})(kw/4)\, [\omega_{HO}^2 - \omega_{CO}^2][\omega_{HO}^2 - \omega_{CO}^2 - (\omega_{CC}^2/2)]^{-1}$$
$$\text{[even } H_2 \text{ sheet mode]} \qquad [43b]$$

The frequency for the even H_2 sheet mode **increases** with juxtaposition to the carbon block.

Finally, consider eq. [42c]. If the right hand side were zero, this would give the frequency for the surface mode of carbon in air, i.e. it would give

$$\omega(w=0)^2 = \omega_{CO}^2 + \omega_{CC}^2/2$$

Since kw<<1, this frequency may be used to evaluate its coefficient $[\varepsilon_H + (\varepsilon_C/\varepsilon_H)]$ to give an approximate solution

$$\omega \approx [\omega_{CO}^2 + \omega_{CC}^2/2]^{1/2} + (\omega_H^2\, \omega_{CC}^2/4)kw[\omega_{CO}^2 + \omega_{CC}^2/2 - \omega_{HO}^2]^{-1}[\omega_{CO}^2 + \omega_{CC}^2/2]^{-1/2} \quad [43c]$$

Note that the carbon surface mode frequency is **increased** by the presence of the hydrogen layer.

To summarize, the relevant zero point frequencies for the surface modes are:

$$\omega = [\omega_{CO}^2 + \omega_{CC}^2/2]^{1/2} \qquad \text{[carbon-air]} \qquad [[23]]$$

$$\omega \approx [\omega_{HO}^2 + \omega_H^2]^{1/2} - \omega_H^2[\omega_{HO}^2 + \omega_H^2]^{-1/2} (kw/4) \quad \text{[odd φ solution H in air]} \qquad [[38b]]$$

$$\omega \approx \omega_{HO} + (\omega_H^2/\omega_{HO})(kw/4) \qquad \text{[even } \varphi \text{ solution H in air]} \qquad [[39b]]$$

$$\omega \approx [\omega_{HO}^2 + \omega_H^2]^{1/2} - \omega_H^2 [\omega_{HO}^2 + \omega_H^2]^{-1/2} (kw/4)\, \xi$$
[odd H_2 sheet mode modified by C] [[43a]]

$$\xi = [\omega_{HO}^2 + \omega_H^2 - \omega_{CO}^2 - \omega_{CC}^2)][\, \omega_{HO}^2 + \omega_H^2 - \omega_{CO}^2 - (\omega_{CC}^2/2)]^{-1}$$

$$\omega \approx \omega_{HO} + (\omega_H^2/\omega_{HO})(kw/4)\, [\omega_{HO}^2 - \omega_{CO}^2]\, [\omega_{HO}^2 - \omega_{CO}^2 - (\omega_{CC}^2/2)]^{-1}$$
[even H sheet modified by C] [[43b]]

$$\omega \approx [\omega_{CO}^2 + \omega_{CC}^2/2]^{1/2} + (\omega_H^2\, \omega_{CC}^2/4)kw[\omega_{CO}^2 + \omega_{CC}^2/2 - \omega_{HO}^2]^{-1}[\omega_{CO}^2 + \omega_{CC}^2/2]^{-1/2}$$
[carbon –air modified by H sheet] [[43c]]

Thus, the binding energy corresponds to the difference frequency formed by summing the first three frequencies (for the infinitely separated components) and subtracting from those the sum of the last three frequencies (for the juxtaposed components):

$$\begin{aligned}\delta\omega = &- (\omega_H^2\, \omega_{CC}^2/4)kw[\omega_{CO}^2 + \omega_{CC}^2/2 - \omega_{HO}^2]^{-1}[\omega_{CO}^2 + \omega_{CC}^2/2]^{-1/2} \\ &+ \omega_H^2\, [\omega_{HO}^2 + \omega_H^2]^{-1/2} (kw/4)(\,\xi\text{-}1) \\ &+ (\omega_H^2/\omega_{HO})(kw/4)\, [1 - [\omega_{HO}^2 - \omega_{CO}^2]\, [\omega_{HO}^2 - \omega_{CO}^2 - (\omega_{CC}^2/2)]^{-1} \quad] \end{aligned} \qquad [44]$$

Where

$$\xi = [\omega_{HO}^2 + \omega_H^2 - \omega_{CO}^2 - \omega_{CC}^2)][\, \omega_{HO}^2 + \omega_H^2 - \omega_{CO}^2 - (\omega_{CC}^2/2)]^{-1}$$

Equation [44] may be rewritten:

$$\begin{aligned}\delta\omega = (kw/4)\, (\omega_H^2\, \omega_{CC}^2)\, [&- \{\omega_{CO}^2 + \omega_{CC}^2/2 - \omega_{HO}^2\}^{-1}\{\omega_{CO}^2 + \omega_{CC}^2/2\}^{-1/2} \\ &+ (1/2)\{\omega_{HO}^2 + \omega_H^2\}^{-1/2}\, \{-\omega_{HO}^2 - \omega_H^2 + \omega_{CO}^2 + (\omega_{CC}^2/2)\}^{-1} \\ &+ (1/2\omega_{HO})\{-\omega_{HO}^2 + \omega_{CO}^2 + (\omega_{CC}^2/2)\}^{-1}] \end{aligned} \qquad [45]$$

The binding energy per unit area is

$$E_1 = \int 2\pi k dk / (2\pi)^2\, (\, h\delta\omega/4\pi) = (h/8\pi^2)\int k dk \delta\omega$$

i.e.

$$\begin{aligned}E_1 = (h/8\pi^2)(k_{max}^3/3)\ \ (w/4)\, (\omega_H^2\, \omega_{CC}^2)\ \ [&- \{\omega_{CO}^2 + \omega_{CC}^2/2 - \omega_{HO}^2\}^{-1}\{\omega_{CO}^2 + \omega_{CC}^2/2\}^{-1/2} \\ &+ (1/2)\{\omega_{HO}^2 + \omega_H^2\}^{-1/2}\, \{-\omega_{HO}^2 - \omega_H^2 + \omega_{CO}^2 + (\omega_{CC}^2/2)\}^{-1} \\ &+ (1/2\omega_{HO})\{-\omega_{HO}^2 + \omega_{CO}^2 + (\omega_{CC}^2/2)\}^{-1}] \end{aligned}$$

On using $k_{max} = (4\pi\, N_s)^{1/2}$ from eq. [14b], we find

$$\begin{aligned}E_1 = (h/8\pi^2)((4\pi\, N_s)^{3/2}/3)\ \ (w/4)\, (\omega_H^2\, \omega_{CC}^2)\ \ [&- \{\omega_{CO}^2 + \omega_{CC}^2/2 - \omega_{HO}^2\}^{-1}\{\omega_{CO}^2 + \omega_{CC}^2/2\}^{-1/2} \\ &+ (1/2)\{\omega_{HO}^2 + \omega_H^2\}^{-1/2}\, \{-\omega_{HO}^2 - \omega_H^2 + \omega_{CO}^2 + (\omega_{CC}^2/2)\}^{-1} \\ &+ (1/2\omega_{HO})\{-\omega_{HO}^2 + \omega_{CO}^2 + (\omega_{CC}^2/2)\}^{-1}] \end{aligned} \qquad [46a]$$

The binding energy per hydrogen molecule is then

$$E_B = E_1/N_s \quad ,$$

$$\begin{aligned}E_B = \ h\pi^{-1/2}\, N_s^{1/2}\ \ (w/12)\, (\omega_H^2\, \omega_{CC}^2)\ \ [&- \{\omega_{CO}^2 + \omega_{CC}^2/2 - \omega_{HO}^2\}^{-1}\{\omega_{CO}^2 + \omega_{CC}^2/2\}^{-1/2} \\ &+ (1/2)\{\omega_{HO}^2 + \omega_H^2\}^{-1/2}\, \{-\omega_{HO}^2 - \omega_H^2 + \omega_{CO}^2 + (\omega_{CC}^2/2)\}^{-1} \\ &+ (1/2\omega_{HO})\{-\omega_{HO}^2 + \omega_{CO}^2 + (\omega_{CC}^2/2)\}^{-1}] \end{aligned} \qquad [46b]$$

Note the strong dependence on the surface density of hydrogen, especially since ω_H^2 is itself proportional to N_s.

6.3 Case 3. A block of isotropic conductor with a thin sheet of hydrogen on a surface

The case of an isotropic conductor of plasma frequency ω_F^2 with a thin sheet of hydrogen on the surface can be obtained directly from the results of the previous sect ion by the replacements:

$$\omega_{CO}^2 => 0 \qquad [47a]$$

$$\omega_{CC}^2 => \omega_F^2 \qquad [47b]$$

Equation [47a] corresponds to the absence of a restoring force on the conduction electrons, except that associated with the plasma properties described by ω_F^2.

By inspection, then, the binding energy of a hydrogen molecule to the isotropic conductor is

$$E_B = h\pi^{-1/2} N_s^{1/2} \ (w/12) (\omega_H^2 \omega_F^2) \ [- \{\omega_F^2/2 - \omega_{HO}^2\}^{-1}\{\omega_F^2/2\}^{-1/2} + (1/2)\{\omega_{HO}^2 + \omega_H^2\}^{-1/2} \{-\omega_{HO}^2 - \omega_H^2 + (\omega_F^2/2)\}^{-1} + (1/2\omega_{HO})\{-\omega_{HO}^2 + (\omega_F^2/2)\}^{-1}] \quad [48]$$

In the limit where

$$\omega_F^2 >> \omega_{HO}^2, \omega_H^2$$

only the hydrogen sheet modes are important. In that case,

$$E_B => h\pi^{-1/2} N_s^{1/2} \ (w/12) \omega_H^2 \ [\{\omega_{HO}^2 + \omega_H^2\}^{-1/2} + (1/\omega_{HO})]$$

When $\omega_{HO}^2 >> \omega_H^2$ – i.e. when the surface density of hydrogen is far from saturation, eq. [88] simplifies further to

$$E_B => h\pi^{-1/2} N_s^{1/2} \ (w/6) \omega_H^2/\omega_{HO} \qquad [49a]$$

As a numerical example, suppose we take the values in Table 2 with the assumed surface density of 1.7×10^{14} cm^{-2} and w = 2.6×10^{-8} cm. Then eq. [49a] gives

$$E_B => 0.018 \text{ eV} \qquad [49b]$$

This is comparable to the oft cited value of 0.04 eV. However, the expression of eq. [49a] is proportional to $N_s^{3/2}$ (since ω_H^2 is itself proportional to N_s). Thus, the magnitude is sensitive to the surface density.

In the next Section, we shall consider binding to graphite itself.

6.4 Case 4. A block of graphite with a thin sheet of hydrogen on a surface

Since graphite is anisotropic, the foregoing results must be modified. In addition, graphite has a dielectric constant different from unity. Both of these effects are accounted for in the Drude

model by introducing a different dielectric constant perpendicular to the graphite planes from that parallel to the planes. Specifically, we shall use the expressions of Table 1:

$$\varepsilon_{\perp}(\omega) = 1 - \omega_C^2 [\omega^2 - \omega_{CO}^2]^{-1} \qquad [[6a]]$$

$$\varepsilon_{\parallel}(\omega) = \varepsilon_{\perp}(\omega) + 4\pi\alpha \qquad [[6b]]$$

$$4\pi\alpha = -\omega_P^2/\omega^2 \qquad [[6c]]$$

The perpendicular dielectric constant is due primarily to the 3 sigma core electrons (assuming that the two 1s electrons are so tightly bound that they do not contribute appreciably.

The parallel dielectric constant contains the polarization contribution of the 3 sigma electrons, and in addition has the polarization term due to the conduction electrons.

Within the graphite, Laplace's equation is no longer satisfied because of the difference of the dielectrics perpendicular and parallel to the surface. Instead the equation for the electrostatic potential φ is

$$d^2\varphi/dx^2 - \gamma^2\varphi = 0 \qquad [50]$$

Where

$$\gamma^2 = (\varepsilon/\varepsilon_{\perp})k^2$$

and where again we have assumed a disturbance of the form $\varphi(x)\exp[i(\omega t - ky)]$.

Note that for a surface mode γ must be real. This imposes the necessary condition:

$\varepsilon_{\parallel}$ and $\varepsilon_{\perp}$ must have the same sign [condition for surface mode] [51]

6.4a Surface mode of a block of graphite and air

Suppose that the graphite block occupies the region $x<0$, and that the air is in the region $x>0$.

Then φ has the form

$$\varphi = A\exp[\gamma x] \qquad x<0 \qquad [52a]$$

$$\varphi = B\exp[-kx] \qquad x>0 \qquad [52b]$$

and the boundary condition at $x = 0$ is

φ continuous [53a]

$$\gamma\varepsilon_{\perp} = -k \qquad [53b]$$

Equation [53b] imposes the requirement

$\varepsilon_{\perp} < 0$ [in order to satisfy continuity of electric displacement] [54]

On combining the conditions of eqs. [51] and [54] we see that the necessary condition for a surface mode is that

Both ε and $\varepsilon_\perp$ must be less than zero [condition for surface mode] [55]

This is a significant condition, because it indicates that the solution cannot be determined by the pi conduction electrons, i.e. a surface mode cannot exist for

$$4\pi\alpha = O(1)$$

for that would give

$$\omega \approx O(\omega_p)$$

and with the typical values of Table 2, this would imply

$$\varepsilon_\perp(\omega) = 1 - \omega_C^2 [\omega^2 - \omega_{CO}^2]^{-1} \approx 1 + \omega_C^2 [\omega_{CO}^2]^{-1} > 0$$

This means that the solution of eq. [53b] is determined primarily by the $\varepsilon_\perp(\omega)$ contribution in both the parallel and perpendicular directions.

From the definitions of the parallel and perpendicular dielectrics, we can write

$$\gamma^2 = [1 + 4\pi\alpha/\varepsilon_\perp] k^2$$

and since the desired surface mode solution is practically determined by $\varepsilon_\perp$, i.e. by $\varepsilon_\perp + 1 \approx 0$, we can treat $4\pi\alpha/\varepsilon_\perp$ as being much less than unity and write approximately

$$\gamma = [1 + 2\pi\alpha/\varepsilon_\perp] k$$

On substituting this in eq. [53b] and iterating on $2\pi\alpha/\varepsilon_\perp$, we find to lowest order

$$\omega \approx [\omega_{CO}^2 + \omega_C^2/2]^{1/2} + (\omega_C^2\omega_p^2/16) [\omega_{CO}^2 + \omega_C^2/2]^{-3/2} \quad [56]$$

This is very similar to the isotropic carbon case, except that the conducting pi electrons increase the zero point frequency of the surface mode.

6.4b Modifications of graphite mode and hydrogen modes for juxtaposition

As with the isotropic carbon case with a thin layer of hydrogen on the surface, assume that φ takes on the forms

$$\varphi = A\exp[kx] \qquad x<0 \qquad [57a]$$

$$\varphi = B\cosh[kx] + C\sinh[kx] \qquad 0<x<w \qquad [57b]$$

$$\varphi = D\exp[-kx] \qquad x>w \qquad [57c]$$

The dispersion relation giving the surface mode zero point oscillation frequencies is obtained from the boundary conditions

φ continuous [58a]

$$\varepsilon_\perp d\varphi(0-)/dx = \varepsilon_H\, d\varphi(0+)/dx \qquad [58b]$$

$$\varepsilon_H\, d\varphi(w-)/dx = d\varphi(w+)/dx \qquad [58c]$$

6.4c Modification to carbon-air surface mode

On using the small argument approximations for the sinh and cosh, we find in the lowest order in kw:

$$\varepsilon_\perp \approx -(k/\gamma)\,[1+\{\varepsilon_H-(1/\varepsilon_H)\}kw] \qquad [59]$$

This equation can be solved by iteration on both $4\pi\alpha/\varepsilon_\perp$ and kw. We find

$$\omega \approx [\{\omega_{CO}^2+\omega_C^2/2\}^{1/2}+(\omega_C^2\omega_p^2/16)\,(\omega_{CO}^2+\omega_C^2/2)^{-3/2}][1-S/RZ] \qquad [60]$$

Where

$$S = (kw/2)\omega_C^2\{\varepsilon_H^{(0)}-(1/\varepsilon_H^{(0)})\}\,[1-(\omega_C^2\omega_p^2/8)\{\omega_{CO}^2+\omega_C^2/2\}^{-2}] \qquad [61a]$$

$$Z = \omega_{CO}^2+\omega_C^2\{2-\omega_p^2\{2\omega_{CO}^2+\omega_C^2\}^{-1}\}^{-1} \qquad [61b]$$

$$R = [2-\omega_p^2\{2\omega_{CO}^2+\omega_C^2\}^{-1}]^2 \qquad [61c]$$

and where

$$\{\varepsilon_H^{(0)}-(1/\varepsilon_H^{(0)})\} \approx -2\omega_H^2[\omega_{CO}^2+(\omega_C^2/2)\{1+(\omega_p^2/4)\{\omega_{CO}^2+\omega_C^2/2\}^{-1}\}-\omega_{HO}^2]^{-1} \qquad [61d]$$

Note that

$$\{\varepsilon_H^{(0)}-(1/\varepsilon_H^{(0)})\} < 0. \qquad [62]$$

so that – as in the isotropic carbon case – the hydrogen sheet actually raises the zero point oscillation frequency of the carbon-air surface mode.

We note also that when $\omega_p \to 0$, eq. [62] reduces to eq. [43c] for the isotropic carbon case, as it should.

6.4d Modification to hydrogen sheet modes

As in the isotropic carbon case, a quadratic equation can be written for ε_H from the boundary conditions:

$$\varepsilon_H^2\,(kw/\varepsilon_\perp)(k/\gamma)+\varepsilon_H[1+(k/\gamma\varepsilon_\perp)]+kw=0 \qquad [63]$$

To lowest order in kw, this has two solutions:

$$\varepsilon_H \approx -(kw)[1+\{k/(\gamma\varepsilon_\perp)\}]^{-1} \qquad \text{[odd } H_2 \text{ sheet solution]} \qquad [64a]$$

$$\varepsilon_H \approx -(1/kw)[1+(\gamma\varepsilon_\perp/k)] \qquad \text{[even } H_2 \text{ sheet solution]} \qquad [64b]$$

The frequency associated with eq. [64a] is:

$$\omega \approx [\omega_{HO}^2+\omega_H^2]^{1/2}[1-(kw/2)\omega_H^2\,[\omega_{HO}^2+\omega_H^2]^{-1}[1+k/(\gamma\varepsilon_\perp)]^{-1} \qquad [65a]$$

and the frequency associated with eq. [64b] is

$$\omega \approx \omega_{HO}[1-(kw/2)\omega_H^2\,[\omega_{HO}]^{-1}[1+(\gamma\varepsilon_\perp/k)]^{-1} \qquad [65b]$$

As with the isotropic carbon case, these two equations can be solved by iteration, in which all the quantities in the coefficients multiplying kw can be evaluated as if kw = 0.

When this is done, we find

$$\omega \approx [\omega_{HO}^2+\omega_H^2]^{1/2} - (kw/2)\omega_H^2 [\omega_{HO}^2+\omega_H^2]^{-1/2} / F \qquad [66a]$$

Where

$$F = 1-[1-\omega_p^2\{\omega_{HO}^2+\omega_H^2\}^{-1}\{1- \omega_C^2(\omega_{HO}^2+\omega_H^2-\omega_{CO}^2)^{-1}\}^{-1}]^{-1/2}[1- \omega_C^2\{ \omega_{HO}^2+\omega_H^2 - \omega_{CO}^2 \}^{-1}]^{-1}$$

[for odd φ hydrogen sheet mode] [66b]

and

$$\omega \approx \omega_{HO} + (kw/2)\omega_H^2 [\omega_{HO}]^{-1} / G \qquad [67a]$$

Where

$$G = 1 + \{1- \omega_C^2(\omega_{HO}^2+\omega_H^2)^{-1}\}\{1- (\omega_p^2/\omega_{HO}^2)(\omega_{HO}^2 - \omega_{CO}^2) (\omega_{HO}^2 - \omega_{CO}^2 - \omega_C^2)^{-1}\}^{1'2}$$

[for even φ hydrogen sheet mode] [67b]

When ω_p-> 0, these equations reduce to the isotropic carbon case, as they must.

To summarize, for graphite, the relevant zero point oscillation frequencies of the surface modes are:

$\omega \approx [\omega_{CO}^2 + \omega_C^2 /2]^{1/2} + (\omega_C^2\omega_p^2/16) [\omega_{CO}^2 + \omega_C^2 /2]^{-3/2}$ graphite in air [[56]]

$\omega \approx [\omega_{HO}^2 + \omega_H^2]^{1/2} - \omega_H^2[\omega_{HO}^2 + \omega_H^2]^{-1/2} (kw/4)$ [odd φ solution H in air] [[38b]]

$\omega \approx \omega_{HO} + (\omega_H^2/\omega_{HO})(kw/4)$ [even φ solution H in air] [[39b]]

$\omega \approx [\{\omega_{CO}^2 + \omega_C^2 /2\}^{1/2} + (\omega_C^2\omega_p^2/16) (\omega_{CO}^2 + \omega_C^2 /2)^{-3/2}][1- S/RZ]$
[C-air modified by H sheet] [[60]]

$S = (kw/2)\omega_C^2\{\varepsilon_H^{(0)}-(1/\varepsilon_H^{(0)})\} [1- (\omega_C^2\omega_p^2/8)\{\omega_{CO}^2+\omega_C^2/2\}^{-2}]$ [[61a]]

$Z = \omega_{CO}^2+\omega_C^2\{2- \omega_p^2\{2\omega_{CO}^2+\omega_C^2\}^{-1}\}^{-1}$ [[61b]]

$R = [2 - \omega_p^2\{2\omega_{CO}^2+\omega_C^2\}^{-1}]^2$ [[61c]]

$\{\varepsilon_H^{(0)} -(1/\varepsilon_H^{(0)})\}\approx - 2\omega_H^2[\omega_{CO}^2 + (\omega_C^2/2)\{1+(\omega_p^2/4)\{\omega_{CO}^2+\omega_C^2/2\}^{-1}\} - \omega_{HO}^2]^{-1}$ [[62]]

$\omega \approx [\omega_{HO}^2+\omega_H^2]^{1/2} - (kw/2)\omega_H^2 [\omega_{HO}^2+\omega_H^2]^{-1/2} / F$ [odd H sheet modified by C] [[66a]]

$F = 1-[1- \omega_p^2\{\omega_{HO}^2+\omega_H^2\}^{-1}\{1- \omega_C^2(\omega_{HO}^2+\omega_H^2 - \omega_{CO}^2)^{-1}\}^{-1}]^{-1/2}[1-\omega_C^2\ \omega_{HO}^2+\omega_H^2 - \omega_{CO}^2 \}^{-1}]^{-1}$
[for odd φ hydrogen sheet mode] [[66b]]

$\omega \approx \omega_{HO} + (kw/2)\omega_H^2 [\omega_{HO}]^{-1} / G$ [even H sheet modified by C] [[67a]]

$$G = 1 + \{1- \omega_C^2(\omega_{HO}^2+\omega_H^2)^{-1}\}\{1- (\omega_p^2/\omega_{HO}^2)(\omega_{HO}^2 - \omega_{CO}^2)\,(\omega_{HO}^2 - \omega_{CO}^2 - \omega_C^2\,)^{-1}\}^{1'2}$$

[for even φ hydrogen sheet mode] [[67b]]

The binding energy corresponding to a surface mode of wave number k is obtained by adding the first three of these frequencies (representing the situation where the components are separated by a very large distance) and subtracting from these the last three frequencies. This gives the difference frequency $\delta\omega$ from which the mode's zero point energy is obtained as $h\delta\omega/4\pi$.

As with the isotropic carbon case, the binding energy per hydrogen molecule is then given by summing over all the surface normal modes in a unit area and dividing by the surface density of hydrogen molecules, i.e.

$$E_B = (1/N_s) \int 2\pi k dk / (2\pi)^2 (h\delta\omega/4) = (1/N_s)\,(h/8\pi)\int k dk \delta\omega \qquad [68]$$

The result is

$$\boxed{E_B = N_s^{1/2}\, h\, (\delta\omega)_o/(3\pi^{1/2})} \qquad [69]$$

Where

$$(\delta\omega)_o = (\omega_C^2\omega_p^2/16)\,(\omega_{CO}^2 + \omega_C^2\,/2)^{-3/2}\,(w/2)[S'/RZ]$$
$$+ (w/4)\,\omega_H^2\,[\omega_{HO}^2+\omega_H^2]^{-1/2}\,[UV-1][UV+1]+ (w/4)(\omega_H^2\,/\omega_{HO}^2)[HK-1][HK+1] \qquad [70a]$$

$$S' = (w/2)\,\omega_C^2\{\varepsilon_H^{(0)}-(1/\varepsilon_H^{(0)})\}\,[\,1- (\omega_C^2\omega_p^2/8)\{\omega_{CO}^2+\omega_C^2/2\}^{-2}] \qquad [70b]$$

$$Z = \omega_{CO}^2+ \omega_C^2\{2- \omega_p^2\{2\omega_{CO}^2+\omega_C^2\}^{-1}\}^{-1} \qquad [70c]$$

$$R = [2 - \omega_p^2\{2\omega_{CO}^2+\omega_C^2\}^{-1}]^2 \qquad [70d]$$

$$\{\varepsilon_H^{(0)}-(1/\varepsilon_H^{(0)})\}\approx - 2\omega_H^2[\omega_{CO}^2 + (\omega_C^2/2)\{1+(\omega_p^2/4)\{\omega_{CO}^2+\omega_C^2/2\}^{-1}\} - \omega_{HO}^2]^{-1} \qquad [70e]$$

$$U = [1- \omega_p^2\{\omega_{HO}^2+\omega_H^2\}^{-1}\,[1- \omega_C^2\{\omega_{HO}^2+\omega_H^2 - \omega_{CO}^2\,\}^{-1}]^{-1}]^{1/2} \qquad [70f]$$

$$V = 1- \omega_C^2\{\omega_{HO}^2+\omega_H^2 - \omega_{CO}^2\,\}^{-1} \qquad [70g]$$

$$H = 1- \omega_C^2\{\omega_{HO}^2 - \omega_{CO}^2\,\}^{-1} \qquad [70h]$$

$$K = [1- (\omega_p^2/\omega_{HO}^2)\,(\omega_{HO}^2 - \omega_{CO}^2)\,\{\omega_{HO}^2-\omega_C^2 - \omega_{CO}^2\,\}^{-1}]^{1/2} \qquad [70i]$$

Note that of the constants in eqs. [70b] -[70i], all are positive except for S'. The significance of this is that the hydrogen layer increases the zero point energy of the carbon-air surface mode, but the carbon decreases the zero point energy of the hydrogen sheet modes. The hydrogen sheet modes are both of $O(\omega_H^2\,/\omega_{HO}\,)$ whereas the carbon surface mode is of $O(\omega_H^2\omega_C^4\omega_p^2\,/\omega_{CO}^7)$. Since ω_{CO} is so large, this indicates that the binding energy is essentially due to the modification of the hydrogen sheet modes by the presence of the graphite.

Figure 7 displays the binding energy per hydrogen molecule (in eV) predicted by eq. [69] plotted vs the surface density of hydrogen molecules (in number of molecules per square centimeter).

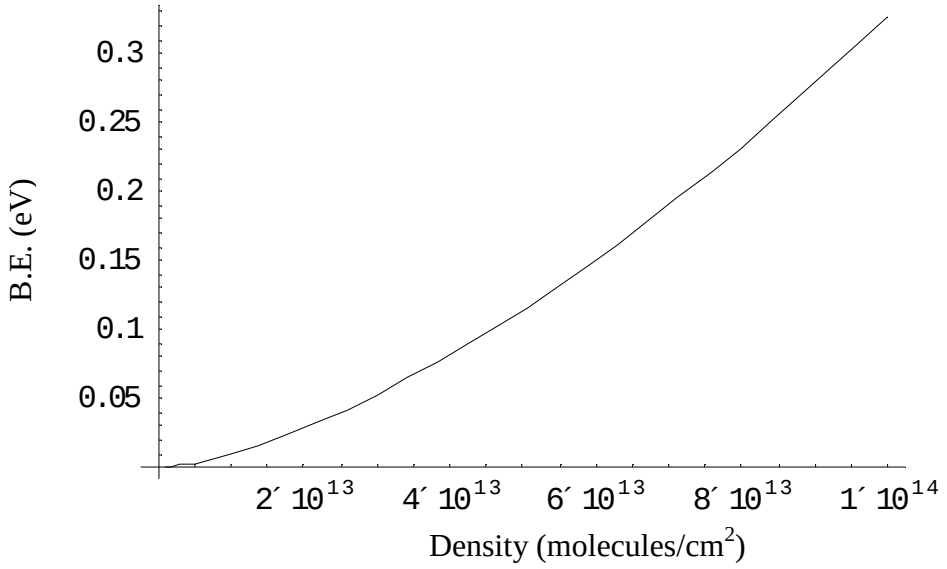

Figure 7. Binding energy vs. the surface density of hydrogen

6.5 Adsorption of hydrogen on graphite

The fractional hydrogen occupancy can be calculated from Langmuir adsorption isotherm derived earlier as:

$$f_H = N / N_s = a_{Langmuir} P [1 + b_{Langmuir} P]^{-1} \quad [[12a]]$$

Where the constants can be expressed in terms of the temperature T and the van der Waals adsorption energy V; specifically:

$$a_{Langmuir} = b_{Langmuir} = h \exp(V/k_B T)[N_s (3m)^{1/2} (k_B T)^{3/2}]^{-1} \quad [[12b]]$$

The Langmuir isotherm equation can be used to plot the pressure, temperature, and adsorption energy dependence of the occupancy of adsorption sites.

To estimate the percentage weight added to the graphite sheet, we need to know the area of the sheet A, the thickness of the sheet d, the surface number density of adsorption sites N_s , and the density ρ. of graphite

Then, if both sides of the sheet are exposed to the hydrogen, and the thickness of the sheet is small compared to the linear dimensions comprising the area A, we have the fractional gain in weight due to the adsorption of the hydrogen:

$$\delta W/W = f_H N_S m(2A) / [\rho A d] = 2 f_H N_S m / [\rho d] \quad [71]$$

7. Discussion

7.1. Comparison with other experiment

There appears to be a range of experimental values reported in the literature for the adsorption energy of molecular hydrogen on a carbon surface. Two examples follow:

Ye [1999] gives a "characteristic chemical potential for hydrogen physisorption" of W = 0.038 eV. [Wang, 1999] quotes an experimental value of W = 910 cal/mole = 910 x 4.18 x 10^7 ergs/ 6.025 x 10^{23} = 631 x 10^{-16} erg/atom = 631 x 10^{-16} / 1.6 x 10^{-12} = 0.039 eV, although they show a range of estimates up to 1293 cal/mole, i.e., W = 0.039-0.055 eV. They also give the depth of the potential well for adsorbing hydrogen to carbon as W = 0.052 eV.

The binding energies calculated here fall in the range of published values, when reasonable assumptions are made about operating pressures and temperatures. For example, the Langmuir isotherm relation of eq. [12] would give a surface density of close to 3x10^{13} molecules per square centimeter at about 30 atmospheres of pressure if the corresponding binding energy were 0.04 eV. It is interesting that Figure 7 shows that a binding energy of close to 0.04 eV corresponds to a surface density of 3x10^{13} cm^{-2}.

At the same time, the binding energies are seen in Figure 7 to depend sensitively on the surface density of the adsorbed hydrogen, and to increase rather dramatically as the surface density increases. This bodes well for high storage densities of hydrogen in graphite-like systems.

7.2. Estimate hydrogen storage capacity

Using equation [71], the hydrogen storage capacity was estimated by comparing the population of the states at the different energies:

Given a binding energy of 0.038 eV (6.1x10^{-19} J)

Ratio = exp [E/k_BT] = exp [6.1 x10^{-19} J/(1.4x10^{-23} J/K x 300 K)] = 4.34 ratio of juxtaposed to isolated sheets

% of hydrogen adsorbed = 4.34/(1 + 4.34) = 81%.

Weight percent of hydrogen = 0.81x (M.W.H_2)/M.W.Carbon = 0.81 x (1 g/mol)/12 g/mol = 6.8%.

7.3 Engineering design considerations

The analysis presented above showed that the predictions of binding energy agree well with the portion of the published data that is more widely accepted. The analytical results on sorption energies and storage capacities will be used for preliminary estimates of required pressures, temperatures, and containment vessel sizes. This should lay the groundwork for a more ambitious program that could lead to an actual engineering prototype for demonstrating the superiority of this type of hydrogen storage system. , we

This section outlines an experimental setup for determining the rate of hydrogen adsorption on sheet of nanofibers carbon materials to prepare a preliminary engineering design of a practical storage device. In addition, a sanity check is performed to be sure that the results are in fair agreement with published data. The proposed setup is given in Figure 8.

Briefly samples of carbon fiber sheets are placed inside a housing where temperature and pressure can be accurately controlled and monitored. To prevent oxidation, the housing will be kept under inert atmosphere by allowing helium from a bottle to fill the chamber. Similarly hydrogen is allowed to fill a container to a specified pressure and room temperature. The sample will be cooled to liquid nitrogen temperatures (77K) where maximum rate of adsorption is expected. Hydrogen will be allowed to fill the chamber at a prescribed pressure until no more drop in hydrogen chamber is observed, i.e. graphite is saturated. The test chamber is then isolated from hydrogen and helium gas and is gradually brought to room temperature. The rise in pressure of the test chamber is directly related to the amount of hydrogen desorbed. A matrix of 9 experiments (three pressures and three temperatures) will be conducted to determine temperature and pressure dependency of adsorption rates.

Schematic of Experimental Set-up for Gaseous Hydrogen Adsorption on Small Carbon Sample

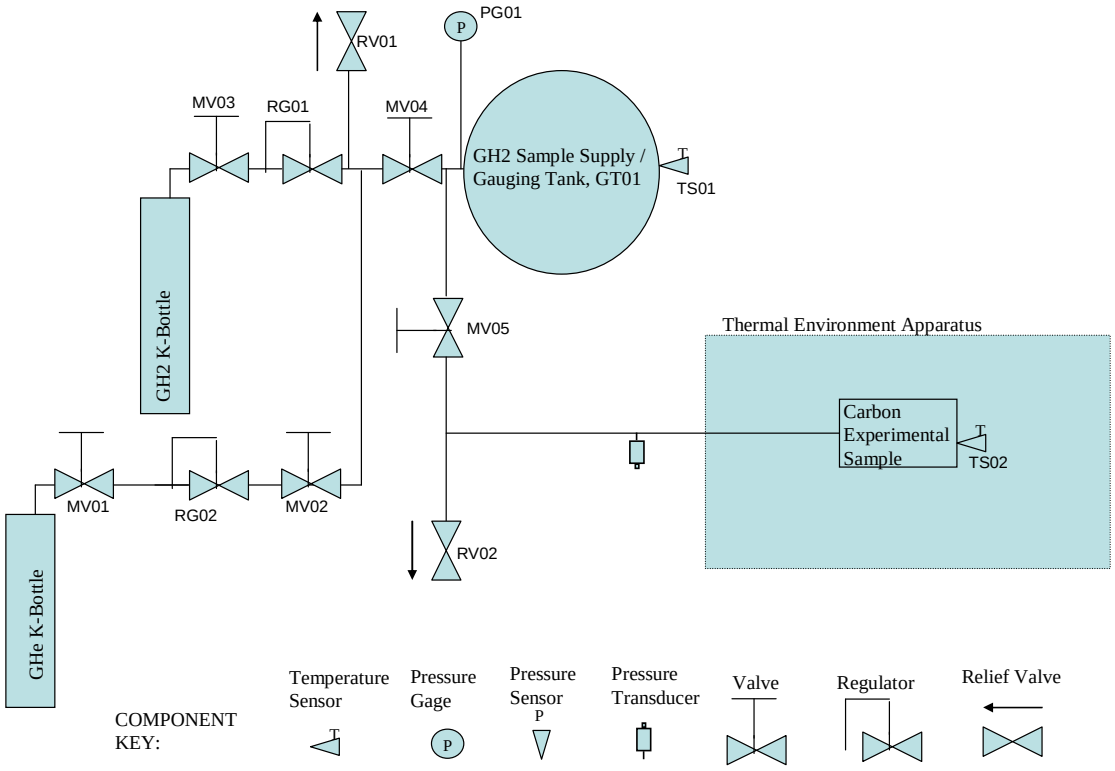

Figure 8. Experimental setup for measuring the rate of adsorption of hydrogen on carbon

8. Future Works

Perhaps the most interesting finding here is that the binding energy per hydrogen molecule depends sensitively on the surface density of the hydrogen molecules: the larger the surface density, the larger the binding energy per hydrogen molecule. This prediction should be testable experimentally and sets the stage for future additional work.

Currently, the experiment envisioned for future work consists of (1) putting some graphite material in a container, (2) filling the evacuated container with hydrogen gas from some known

pressure [e.g. atmospheric pressure]; (3) measuring the pressure in the vessel after the hydrogen is introduced at three different temperatures.

From the change in pressure with temperature, the binding energy can be deduced from a modified Langmuir isotherm equation in which the binding energy itself is dependent on the surface density of adsorbed hydrogen.

Commercial sources are available for three types of relatively inexpensive graphite material: (1) graphite flakes, (2) graphite powder, and (3) nanotube soot. Of these, the most promising is the third, since it has a much larger surface area to adsorb the hydrogen than the first two.

9. References

1. Ahn, C.C, Ye, Y., Ratnakumar, B.V., Whitlam, C., Bowman, R.C. and Fultz, B., "Hydrogen desorption and adsorption measurements on graphite nanofibers," *Appl. Ph. Lett.* **73** (23) 3378-3380 (1998)
2. Atkinson, K., Roth, S., Hirscher, M., and Grunwald, M., "Carbon nanostructures: an efficient hydrogen storage medium for fuel cells," Fuel Cells Bulletin No. 38, Elsevier (2002).
3. Baker, R. Terry K, and Rodriguez, N. M., "High performance carbon filament structures", U.S. Patent **5,**618, 875 (1997).
4. Chang, D. B., and Drummond, J. E., "Plasma effects in annulene molecules", The Journal of Chemical Physics **52**, 4533-4544 (1970).
5. Chang, D B, Cooper, R.L., Drummond, J.E., and Young, A.C., "Van der Waals Attraction between Two Conducting Chains," *Physics Letters* A37A. 311-312 (1972).
6. CRC Handbook of Chemistry and Physics. B0Ca Raton: CRC Press, Inc., B-12 (1984).
7. Eyring, H., Walter, J., and Kimball, G. F., Quantum Chemistry. New York: Wiley and Sons, Inc. (1944).
8. Landau L.D. and E.M. Lifshitz, "Statistical Physics", Reading, Mass: Addison-Wesley Publishing Company, Section 126 (1969).
9. Meregalli, V. and Parinello, M., "Review of theoretical calculations of hydrogen storage in carbon-based materials", Appl. Phys. A72(2), 143-146 (2001).
10. Rodriguez, N. M., and Baker, R. Terry K., "Storage of hydrogen in layered nanostructures", U.S. Patent 5,653, 951 (1997).
11. Salem, L., "Attractive forces between long saturated chains at short distances", *J. Chem. Phys.* **37**, 2100 (1962)
12. Slater, J.C., Insulators, Semiconductors and Metals, Quantum Theory of Molecules and Solids Volume 3. New York: McGraw-Hill Book Company (1967).
13. Wang, Q. and J.Hanson, J.K., "Molecular Simulation of Hydrogen Adsorption in Single-Walled Carbon Nanotubes and Idealized Carbon Slit Pores", *J Chem Phys* vol 110, 577 (1999).
14. Wang, Q., and J.K. Johnson, "Hydrogen adsorption on graphite and in carbon slit pores from path integral simulations," *Molecular Physics*, **95**, 299-309 (1998)
15. Yasuda, Y., "The Drude Model Calculation" *J. Phys. S0C. Japan* 26, 163 (1969)
16. Ye, Y., Ahn, C.C., Witham, C., Fultz, B. , Liu, J. , Rinzler, A.G. , Colbert, D., Smith, K.A., and Smalley, R.E., "Hydrogen adsorption and c0Hesive energy of single-walled carbon nanotubes," *Applied Physics Letters* **74**, 2307 (1999)
17. Zwanzig, R., "Two Assumptions in the Theory of Attractive Forces Between Long Saturated Chains", *J. Chem. Phys.* 39,2251 (1963).

Appendix A

The fluctuation-dissipation theorem states that for a system with a Hamiltonian

$$H = H^{(o)} + \Sigma F_i(t)\, Q_i \qquad [A\text{-}1]$$

where $H^{(o)}$ is the unperturbed Hamiltonian of the system and the term $\Sigma F_i(t)\, Q_i$ represents the interaction of the system observables Q_i with external driving forces $F_i(t)$, the spectra $G_{ij}(\omega)$ of the Q_i's in thermal equilibrium may be expressed in terms of the response functions of the system which gave the time rates of change of the expectation values of the system observables $<dQ_i/dt>$ which result when external forces $F_i(t)$ are applied.

If the time-Fourier-transforms of $<dQ_i/dt>$ and $F_i(t)$,

$$\alpha_j(\omega) = [1/(2\pi)^{1/2}] \int dt\, \exp[-i\omega t] <dQ_i/dt> \qquad [A\text{-}2]$$

$$\gamma_j(\omega) = [1/(2\pi)^{1/2}] \int dt\, \exp[-i\omega t]\, F_i(t) \qquad [A\text{-}3]$$

are related by the response function $Y_{ij}(\omega)$,

$$\alpha_j(\omega) = \Sigma\, Y_{ij}(\omega)\gamma_i(\omega)$$

then the fluctuation-dissipation theorem states that the power spectra $G_{ij}(\omega)$, defined as the Fourier transforms of the correlation functions $(1/2) < [Q_i, Q_j(T)]_+ >$ of the observables Q_i and Q_j in thermal equilibrium,

$$G_{ij}(\omega) = [1/(2\pi)^{1/2}] \int dt\, \exp[-i\omega t]\, (1/2) < [Q_i, Q_j(T)]_+ > \qquad [A\text{-}4]$$

Are given in terms of the blackbody function

$$E(\omega,\beta) = (h\omega/4\pi) \coth (h\beta\omega/4\pi) \qquad [A\text{-}5]$$

and $Y_{ij}(\omega)$ by

$$^{(s)}G_{ij}(\omega) = -(2/\pi)^{1/2} [E(\omega,\beta)/\omega^2]\, \mathrm{Re}\, ^{(s)}Y_{ij}(\omega) \qquad [A\text{-}6a]$$

$$^{(a)}G_{ij}(\omega) = -i\,(2/\pi)^{1/2} [E(\omega,\beta)/\omega^2]\, \mathrm{Im}\, ^{(a)}Y_{ij}(\omega) \qquad [A\text{-}6b]$$

In these equations, the superscripts (s) and (a) refer to the portions of the function which are symmetrical and asymmetrical, respectively, in the subscripts and j., and

$$\beta = (1/k_B T)$$

where k_B is Boltzmann's constant and T is the temperature.

Consider, then, a damped harmonic oscillator for which the equation of motion is

$$Md^2x/dt^2 = -Kx - M\upsilon dx/dt + F \qquad [A\text{-}7]$$

Here, M denotes the mass of the oscillator, x is its displacement, K is the restoring force constant, υ is the frictional drag coefficient that describes the dissipative force on the oscillator, and F is the external force acting on the oscillator.

For this oscillator, the response function is simply

$$Y(\omega) = (1/M)\,[(\omega_o^2 - \omega^2) - i\omega\upsilon]^{-1} \qquad \text{[A-8]}$$

where

$$\omega_o^2 = K/M$$

It is straightforward to apply equation [14] to this response function. In the limit where

$$\upsilon << \omega_o$$

and

$$h\beta\omega_o/4\pi) >> 1$$

the equations simplify considerably. Specifically,

$$E(\omega,\beta) = (h\omega/4\pi)\coth(h\beta\omega/4\pi) \Rightarrow (h\omega/4\pi) \qquad \text{[A-9]}$$

and we find that the average energy <W> of the oscillator is simply

$$\langle W\rangle = (\tfrac{1}{2}\,M)\langle(dx/dt)^2\rangle + (\tfrac{1}{2}\,K)\langle x^2\rangle = h\omega_o/4\pi \qquad \text{[A-10]}$$

This is the zero point energy result assumed in the previous section.

An interesting situation develops, however, in the situation where

$$\omega_o = 0 \qquad \text{[Special case were there is no restoring force]}$$

In that case, the main contribution comes from ω for which

$$h\beta\omega/4\pi << 1$$

in which case,

$$E(\omega,\beta) = (h\omega/4\pi)\coth(h\beta\omega/4\pi) \Rightarrow (1/\beta) = k_B T$$

In that special case,

$$(\tfrac{1}{2}\,M)\langle(dx/dt)^2\rangle = (\upsilon k_B T/\pi)\int d\omega\,[\omega^2 + \upsilon^2]^{-1} = k_B T/2 \qquad \text{[A-11]}$$

When the restoring force disappears, the zero point energy $h\omega_o/4\pi$ is replaced by the thermal energy $k_B T/2$.

It is interesting that the theorem shows that in the first approximation it is not necessary to include dissipation in the expressions for the response functions. Accordingly, in the following, we shall ignore the resistivity in the conducting material.